

PAPER • OPEN ACCESS

Modeling techniques for kinematic analysis of a six-axis robotic arm

To cite this article: R Guida *et al* 2019 *IOP Conf. Ser.: Mater. Sci. Eng.* **568** 012115

View the [article online](#) for updates and enhancements.



IOP | ebooks™

Bringing you innovative digital publishing with leading voices to create your essential collection of books in STEM research.

Start exploring the **collection** - download the first chapter of every title for free.

Modeling techniques for kinematic analysis of a six-axis robotic arm

R Guida¹, M C De Simone^{2*}, P Dašić³ and D Guida²

¹ MEID4 S.r.l., Fisciano 84084, Italy

² The University of Salerno. Via Giovanni Paolo II, 84084 Fisciano, Italy

³ High Technical Mechanical School of Professional Studies, Trstenik, 37240, Serbia

mdesimone@unisa.it

Abstract. The purpose of this analysis is to evaluate the effectiveness of different modeling techniques for a COMAU six-axis robot arm. The robot manipulator represents one of the most used robots in the mechanical industry. For robots, with a high number of degrees of freedom, to obtain a kinematic model, Denavit-Hartenberg parameters allow representing geometric transformations in the Euclidean space through the minimum number of parameters. Furthermore, the use of detailed multibody models and the use of sophisticated tools like the Robotics Toolbox System, allow performing, in a very efficient way, inverse kinematic analysis and trajectory planning to control the robot move from one configuration to another.

1. Introduction

According to the International Federation of Robotics (IFR), the increased speed of development of robotics is mainly benefited by the progress of off-the-shelf, low-cost equipment, software packages or codes almost ready to use, developments expected by the industry and active communities in the field [1]. To design a robot, it is essential to establish the optimal configuration by analyzing its kinematic behavior. There are many optimization techniques in literature for the design of optimal configurations. As reported in Cesconeto and Perondi (2019), optimum strategies must be evaluated to evaluate the optimum length of single links and joint angular limits to design an arm with the best possible kinematic performance within a desired design-defined workspace [2]. It is important for developers and implementers, to be aware of the available platforms, methods, algorithms, hardware components, that are most used, underlying physical and numerical paradigms [3-4]. All these aspects have an impact on safety and goal reaching motion; that is why we are interested in a good understanding of modeling techniques for kinematic and dynamic analysis and expertise on software architectures for robot application, as demonstrated by the growing number of developers of open-source systems for robotics as in the case of the ROS-Gazebo robot platform [5-6]. This paper represents a preliminary study to evaluate the effectiveness of different modeling systems for a subsequent experimental activity on the retrofitting of an industrial robot COMAU Smart Six6-1.4 of the Applied Mechanics laboratory [7-8].

2. The COMAU Smart Six 6-1.4

The COMAU Smart SiX 6-1.4 is a manipulator robot produced by the company Comau (Consorzio MACchine Utensili), an Italian multinational company that is part of FCA Group. It develops and realizes the automation process and solutions to meet specific manufacturing needs for industries ranging from railway, heavy industrial, renewable energy, and automotive [9]. The manipulator consists



of 6 links, that form an open kinematic chain. Every joint represents a cylindrical hinge (shaped by a revolute joint). The motion is led by brushless DC electric motors (BLDC), also known as electronically commutated motors. The BLDC motors present various advantages: they have a high power to weight ratio, high speed, and electronic control. The motion transmission takes place by means of gears (for the axes 1, 2, 3, 4) and using a belt (for the axes 5, 6). The belt transmission also has a Harmonic Drive, a strain wave gear. The joints of the robot have end stops, that can be software or mechanical [10]. In Fig. 3, the technical specifics of the robot are reported. Before using the robot is necessary to calibrate it. The calibration consists in bringing the joints in a known position to guarantee the correct repetition of the programmed cycles [11]. The two possible different kinds of calibration are:

- Precise calibration, used before cycles that need to be very accurate;
- Reference notches calibration, used in other cases, this kind of calibration is faster but more inaccurate.

The robot is governed by an algorithm that performs a position control. The control system uses PID controllers (Proportional-Integral-Derivative control) that uses the encoders of the 6 axes to compare the actual position of the joints to the reference position [12].

The robot has its programming language, the PDL2, language is very similar to Pascal, an object-oriented programming paradigm. The code can be uploaded by using C4G, a controller given by the company, or using a PC, linked thanks to a LAN connection. As default every motion law is built using a trapezoidal trajectory, but this setting could be changed.

3. Robot Arm Kinematics

To proceed with the analysis of the anthropomorphic manipulator, the reference frame 0 is chosen with the origin at the intersection of z_0 and z_1 ($d_1 = 0$), and z_1 and z_2 are parallel as reported in Fig. 1a). Choosing x_1 and x_2 along the direction of the respective link in order to make null every d_i .

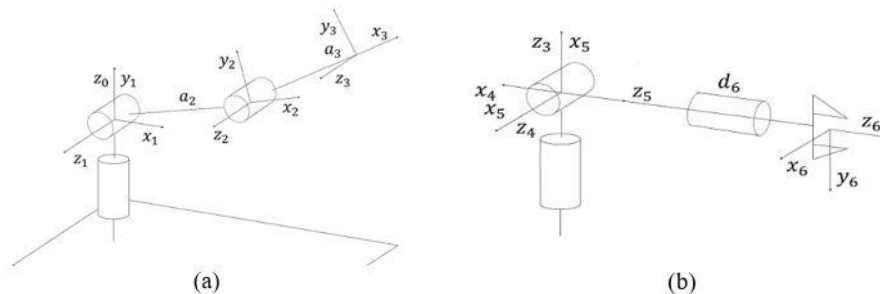


Figure 1. Reference frames used for the kinematic analysis: (a) frame references used for links 1, 2 and 3, (b) frames references used for links 4, 5, and 6.

In (1), (2) and (3), are reported the transformation matrices for link 1, 2, and 3, respectively.

$$A_1^0(\theta_1) = \begin{bmatrix} c_1 & 0 & s_1 & 0 \\ s_1 & 0 & -c_1 & 0 \\ 0 & 1 & 0 & 0 \\ 0 & 0 & 0 & 1 \end{bmatrix} \quad (1)$$

$$A_2^1(\theta_2) = \begin{bmatrix} c_2 & 0 & s_2 & 0 \\ s_2 & 0 & -c_2 & 0 \\ 0 & 1 & 0 & 0 \\ 0 & 0 & 0 & 1 \end{bmatrix} \quad (2)$$

$$A_3^2(\theta_3) = \begin{bmatrix} c_3 & 0 & s_3 & 0 \\ s_3 & 0 & -c_3 & 0 \\ 0 & 1 & 0 & 0 \\ 0 & 0 & 0 & 1 \end{bmatrix} \quad (3)$$

The direct kinematic function is reported below:

$$T_3^0(q) = A_1^0 A_2^1 A_3^2 = \begin{bmatrix} c_1 c_{23} & -c_1 s_{23} & s_1 & c_1(a_2 c_2 + a_3 c_{23}) \\ s_1 c_{23} & -s_1 s_{23} & -c_1 & s_1(a_2 c_2 + a_3 c_{23}) \\ s_{23} & c_{23} & 0 & a_2 s_2 + a_3 s_{23} \\ 0 & 0 & 0 & 1 \end{bmatrix} \quad (4)$$

with $q = [\theta_1 \ \theta_2 \ \theta_3]^T$ the first, second and third joint variables. The second part of the kinematic study consist in considering exclusively the spherical wrist. In this case the first link is indicated with the number 4. Since the three axes of rotation intersect all in the same point, once identified z_3, z_4 and z_5 and defined x_3 , the direction of x_4 and x_5 are indeterminate. Such directions are chosen as reported in Fig. 1b).

$$A_4^3(\theta_4) = \begin{bmatrix} c_4 & 0 & -s_4 & 0 \\ s_4 & 0 & c_4 & 0 \\ 0 & -1 & 0 & 0 \\ 0 & 0 & 0 & 1 \end{bmatrix} \quad (5)$$

$$A_5^4(\theta_5) = \begin{bmatrix} c_5 & 0 & s_5 & 0 \\ s_5 & 0 & -c_5 & 0 \\ 0 & 1 & 0 & 0 \\ 0 & 0 & 0 & 1 \end{bmatrix} \quad (6)$$

$$A_6^5(\theta_6) = \begin{bmatrix} c_6 & -s_6 & 0 & 0 \\ s_6 & c_6 & 0 & 0 \\ 0 & 0 & 1 & d_6 \\ 0 & 0 & 0 & 1 \end{bmatrix} \quad (7)$$

Considering the transformation matrices reported in (5), (6) and (7), the direct kinematic function assumes the following form:

$$T_6^0(q) = A_1^0 A_2^1 A_3^2 = \begin{bmatrix} c_1 c_{23} & -c_1 s_{23} & s_1 & c_1(a_2 c_2 + a_3 c_{23}) \\ s_1 c_{23} & -s_1 s_{23} & -c_1 & s_1(a_2 c_2 + a_3 c_{23}) \\ s_{23} & c_{23} & 0 & a_2 s_2 + a_3 s_{23} \\ 0 & 0 & 0 & 1 \end{bmatrix} \quad (8)$$

R_6^3 matrix, which can be extracted from T_6^3 , coincides with the rotation matrix of the Euler angles, ie θ_4, θ_5 and θ_6 compose the set of Euler ZYZ angles with respect to the reference frame O_3-x_3, y_3, z_3 . Finally, for describing the COMAU Smart Six configuration the kinematic function is defined from link 0 to link 6.

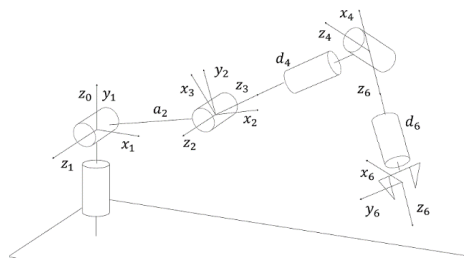


Figure 2. Reference frames used for the kinematic analysis of the anthropomorphic robot.

It cannot be obtained by product of the two matrices T_3^0 and T_6^3 since the 3rd frame of the manipulator cannot coincide with the 3rd frame of the wrist. The resolution of this problem follows two paths, the first is to impose a constant transformation between the two reference frames in order to overlap them, the second is to follow the procedure of D-H for all reference frames (see Fig. 2).

Doing so, we obtain the following parameters: rows 3 and 4 are different from the previously highlighted parameters, so the matrices of homogeneous transformation change, as reported in eq. (9) and (10).

$$A_3^2(\theta_3) = \begin{bmatrix} c_3 & 0 & s_3 & 0 \\ s_3 & 0 & -c_3 & 0 \\ 0 & 1 & 0 & 0 \\ 0 & 0 & 0 & 1 \end{bmatrix} \quad (9)$$

$$A_4^3(\theta_4) = \begin{bmatrix} c_4 & 0 & -s_4 & 0 \\ s_4 & 0 & c_4 & 0 \\ 0 & -1 & 0 & d_4 \\ 0 & 0 & 0 & 1 \end{bmatrix} \quad (10)$$

The other matrices instead, remain the same. After calculating the direct kinematics function, the position and the orientation of the tool axis can be expressed by defining the values of p^0 , n^0 , s^0 and a^0 .

$$p^0 = \begin{bmatrix} a_2c_1c_2 + d_4c_1s_{23} + d_6(c_1(c_{23}c_4s_5 + s_{23}c_5) + s_1s_4s_5) \\ a_2s_1c_2 + d_4s_1s_{23} + d_6(s_1(c_{23}c_4s_5 + s_{23}c_5) + c_1s_4s_5) \\ a_2s_2 - d_4c_{23} + d_6(s_{23}c_4s_5 - c_{23}c_5) \end{bmatrix} \quad (11)$$

$$n^0 = \begin{bmatrix} c_1(c_{23}(c_4c_5c_6 - s_4s_6) - s_{23}s_5c_6) + s_1(s_4c_5c_6 + c_4s_6) \\ s_1(c_{23}(c_4c_5c_6 - s_4s_6) - s_{23}s_5c_6) - c_1(s_4c_5c_6 + c_4s_6) \\ s_{23}(c_4c_5c_6 - s_4s_6) - s_{23}s_5c_6 \end{bmatrix} \quad (12)$$

$$s^0 = \begin{bmatrix} c_1(-c_{23}(c_4c_5c_6 + s_4s_6) + s_{23}s_5c_6) + s_1(-s_4c_5c_6 + c_4s_6) \\ s_1(-c_{23}(c_4c_5c_6 + s_4s_6) + s_{23}s_5c_6) - c_1(-s_4c_5c_6 + c_4s_6) \\ -s_{23}(c_4c_5c_6 + s_4s_6) - c_{23}s_5c_6 \end{bmatrix} \quad (13)$$

$$a^0 = \begin{bmatrix} c_1(c_{23}c_4c_5c_6 - s_{23}c_5) + s_1s_4s_5 \\ s_1(c_{23}c_4c_5c_6 + s_{23}c_5) + s_1s_4s_5 \\ s_{23}(c_4c_5c_6 - s_4s_6) - s_{23}s_5c_6 \end{bmatrix} \quad (14)$$

4. Numerical Analysis

The aim of this paper, is to test the effectiveness of the methods presented for performing inverse kinematic analysis of the COMAU Smart Six 6-1.4. As a reference, we chose to create a multibody model of the robot by importing a three-dimensional CAD model of the robot under analysis into SimScape, the multibody environment of Simulink [14]. The use of detailed geometries allows to have a good model in which mass distribution is considered making the dynamic study much more accurate. In this paper the multibody model has been used in the kinematic analysis as a reference target. The Robotics Toolbox (RTB), developed by Peter Corke, is a MATLAB toolbox which allows to simulate the operation of terrestrial robots and of robotic arms. The original release dates back to the early 90s and supported exclusively the simulation of robotic arms, represented as one serial structure of links and to perform direct and inverse kinematic and dynamic analysis [13]. The Toolbox is based on a general method of representation of the kinematics and the dynamics of robots. The robot, as previously explained, is a manipulation with six degrees of freedom definite through six revolute joints. Such configuration is described by the string "RRRRRR" where the letters define the type of joint: (R) revolute or (P) prismatic. To define a new robot inside the Toolbox you must first of all define the Denavit-Hartenberg parameters of the robot in question, which depend not only on the type of robot but on the structural parameters reported in Fig. 2. Once the structural parameters have been selected, the various links of which it is composed are defined. Several values were used for testing the robotics toolbox. In Fig. 4.a) is reported the result of a simulation, conducted by using the Robotics Toolbox. Such toolbox, offers the possibility to take into account the external forces acting on the joints. To do so, it is possible to use the itorque, coriolis and gravload instructions which allow, respectively, to evaluate the inertial, the Coriolis and the gravitational terms.

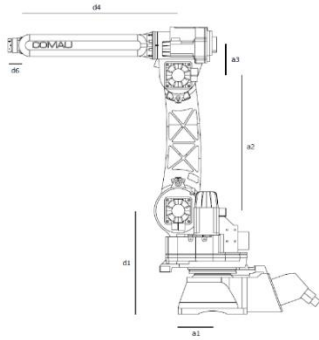
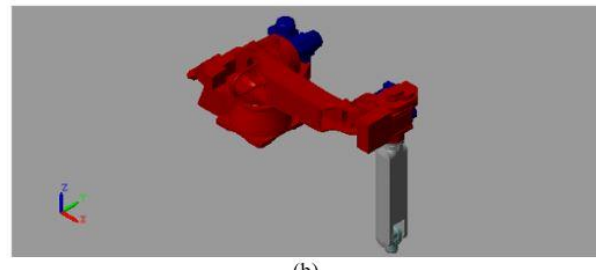
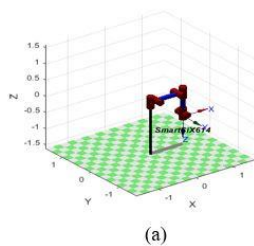


Table 1. D-H parameters

j	theta	d	a	alpha	offset
1	0.15	0.45	0.15	1.5708	0
2	0.59	0	0.59	0	0
3	0.13	0	0.13	1.5708	0
4	0.007	0.674	0	-1.5708	0
5	0.45	0	0	1.5708	0
6	0.64707	0.095	0	0	0

Figure 3. Geometric parameters and values of the D-H parameters used for the robotics toolbox.

The use of such function allows to create a mathematical model more coherent with reality, to create a more precise control of motion and position, but these details do not affect the study of the kinematics. Robotics Toolbox also provides tools for calculating differential kinematics, such as the `tr2jac` function, which outputs the Jacobian matrix to obtain the velocity between two links connected by a homogeneous transformation matrix. In Fig. 5, is reported the behaviour of the robot for the configuration reported previously. Such configurations, will be compared with multibody model described in the following section. The SimScape multibody simulation environment is a multi-domain environment in which it is possible to make different systems interact in a simple way. Starting from a three-dimensional geometry it is possible to obtain a multibody model in which the mass distribution is much more accurate and therefore the answer will be much more precise in simulation. For our application, the geometry of the anthropomorphic robot was replicated by using Solidworks 3D CAD modeller and thanks to the SimMechanics Link Tool, imported into the SimScape multibody simulation environment [14]. In this environment it is possible to model the actuators and the sensors by an electrical and electronic point of view in order to achieve a much more accurate model of the system [15]. In Fig. 4.b), is reported the simulation conducted on the multibody model for the same configurations.

**Figure 4.** Kinematic simulation of the Comau Smart SiX 6-1.4: (a) robotics toolbox (b) Simscape.

In table 1, are reported the position of the end effector for the models with the percentage error.

5. Conclusions

The goal of the paper is to test different modelling techniques in order to evaluate the effectiveness of the several models for describing a specific anthropomorphic manipulator, the COMAU Smart SiX-6.14 for a subsequent retrofitting activity [16]. The analytical model and the multibody model were evaluated by using Matlab software, which allowed us to perform various tests in order to evaluate the consistency of the results very quickly [17]. For this study we chose to test the modelling techniques by using the Denavit-Hartenberg parameters, the robot toolbox and a rigid multibody model obtained using Solidworks and the Simscape environment. The errors made by the models used for this analysis ranged from 5% to 8%, however, remaining below 10% and thus showing a validity of all the proposed models.

Table 2. Comparison of the proposed methods by using the multibody model as a reference

Configuration	Multibody model	Denavit-Hartenberg	error	Robotics Toolbox	error
$q_z = [0 \ 0 \ 0 \ 0 \ 0 \ 0]$	[0.87 0 -0.27]	[0.87 0 -0.27]	5%	[0.87 0 -0.27]	5%
$q_r = [\frac{\pi}{2} \ 0 \ 0 \ 0 \ 0 \ 0]$	[0.87 0 1.17]	[0.892 0 1.17]	5%	[0.892 0 1.17]	5%
$q_s = [0 \ \frac{\pi}{2} \ 0 \ 0 \ 0 \ 0]$	[1.465 0 0.58]	[1.482 0 0.58]	5%	[1.482 0 0.58]	5%
$q_n = [\frac{\pi}{4} \ 0 \ 0 \ \frac{\pi}{4} \ 0 \ 0]$	[1.19 0 0.501]	[1.12 0 0.506]	5%	[1.211 0 0.501]	6%

References

- [1] Cammarata A 2015 Optimized design of a large-workspace 2-DOF parallel robot for solar tracking systems *Mechanism and Machine Theory*. **83** 175-186.
- [2] Cesconeto E M and Perondi E A 2019 Development of a hydraulic robotic arm – Determination of the kinematic parameters *Lecture Notes in Electrical Engineering*. **505** 537-544.
- [3] Sahu P K *et al.* 2019 A Heuristic Comparison of Optimization Algorithms for the Trajectory Planning of a 4-axis SCARA Robot Manipulator *Advances in Intelligent Systems and Computing*. **711** 569-582.
- [4] Fenucci A *et al.* 2016 An off-line robot motion planning approach for the reduction of the energy consumption. In *IEEE International Conference on Emerging Technologies and Factory Automation, ETFA, 2016-November*.
- [5] Colucci F, De Simone M C and Guida D 2020 TLD Design and Development for Vibration Mitigation in Structures *Lecture Notes in Networks and Systems*. **76** 59-72.
- [6] Živković M, Dašić P and Petrović Z 2019 Influence of New Technologies on Higher Energy Efficiency of Hydrostatic Devices and Systems *Lecture Notes in Networks and Systems*. **42** 386-396.
- [7] Pappalardo C M and Guida D 2018 On the Computational Methods for the Dynamic Analysis of Rigid Multibody Mechanical Systems *Machines*. **6(2)** 20.
- [8] De Simone M C, Rivera Z B and Guida D 2018 Obstacle avoidance system for unmanned ground vehicles by using ultrasonic sensors *Machines*. **6 (2)** 18.
- [9] Knox J 2017 Comau leads the digital transformation in the industrial world together with Microsoft and ICONICS *Automotive Industries AI*. **197 (4)**.
- [10] Nagpal N *et al.* 2019 Tracking control of 4-DOF robotic arm using krill herd-optimized fuzzy logic controller *Advances in Intelligent Systems and Computing*. **697** 629-643.
- [11] Lin Y *et al.* 2018 A computationally efficient and robust kinematic calibration model for industrial robots with kinematic parallelogram. In: *2017 IEEE International Conference on Robotics and Biomimetics, ROBIO 2017, 2018-January*
- [12] Trapani S and Indri M 2018 Task modeling for task-oriented robot programming. In: *IEEE International Conference on Emerging Technologies and Factory Automation, ETFA*. 1-8.
- [13] Corke P I 1996 A robotics toolbox for MATLAB *IEEE Robotics & Automation Magazine*. **3(1)** 24-32.
- [14] Concilio A *et al.* 2017 A new semi-active suspension system for racing vehicles *FME Transactions*. **45(4)** 578-584.
- [15] Gao G *et al.* 2018 Structural parameter identification for 6 DOF industrial robots *Mechanical Systems and Signal Processing*. **113** 145-155.
- [16] Pappalardo C M, De Simone M C and Guida D 2019 Multibody modeling and nonlinear control of the pantograph/catenary system *Archive of Applied Mechanics*.
- [17] Francesco P and Paolo G G 2017 AURA: An Example of Collaborative Robot for Automotive and General Industry Applications *Procedia Manufacturing*. **11** 338-345.